La Metallurgia Italiana
International Journal of the Italian Association for Metallurgy

AA new approach on hydrogen permeation for enamelling grade steels

edited by: C.M. Belardini, R. Valentini, M. De Sanctis, B.D. Monelli

Hydrogen diffusivity is strongly affected by the presence of traps, which are defects of the metal matrix that offer a location for hydrogen atoms with a lower energy state than regular interstitial lattice sites. The study of hydrogen diffusion is relevant for multiple different reasons, according to the specific application that is considered. In the context of enamelling grade steels, hydrogen is the cause of the defect known as fishscaling, or the detachment of enamel pieces from the metal surface. Study of hydrogen trapping and diffusion is part of the process of understanding fishscaling, since for many materials, a strong link was found between high diffusivity and fishscaling susceptibility. This study is performed with the use of hydrogen permeation tests, but the interpretation of permeation data is not straightforward because of the trapping effect. In this paper, temperature programmed desorption tests were performed on enamelling grade interstitial free steels to provide an initial understanding of the type of traps expected. Then hydrogen permeation tests were performed to further characterize the trapping parameters of the materials. Common methods to estimate the apparent diffusivity were compared, and the experimental curves were reconstructed using McNabb and Foster's trapping and diffusion model. Finally, a simple method is proposed that may lead to simple empiric formulae to estimate trapping parameters from permeation tests for specific families of materials, possibly overcoming the issues inherent in employing the common and simplified apparent diffusivity approach.

INTRODUCTION

Enamelling steel products are commonly used for domestic and sanitary appliances or in architecture. Enamelling steels have excellent resistance to typical conditions expected for their applications (corrosion protection, resistance to thermal shock and fire, abrasives...) and generally good formability. They comply with hygiene and food safety requirements and allow for a vast range of surface aesthetics [1, 2]. Enamel is applied on the steel in one or more layers and bonded to it by one or more firing rounds in controlled high-temperature conditions. During the firing processes, excessive humidity may cause hydrogen entry into the specimen. Hydrogen, being the smallest atom, can easily enter into the metal matrix and diffuse even at room temperature. If excessive hydrogen enters the material a defect known as fishscaling can occur, which is an irregular detachment of enamel from the surface. Therefore, to assess the fishscaling resistance of enamelling steels, the knowledge of the diffusive proper-

C.M. Belardini, R. Valentini, M. De Sanctis, B.D. Monelli
Università di Pisa
carlomaria.belardini@phd.unipi.it

S. Corsinovi
Letomec s.r.l.

M. Levaux
ArcelorMittal

ties of hydrogen in said steels is a fundamental step [3, 4, 5].

Hydrogen occupies interstitial sites in the metal matrix, and thermally activated random jumps cause its diffusion along the hydrogen concentration gradient. To study hydrogen diffusion, hydrogen permeation tests are the most direct experimental technique available [6, 7, 8]. During the test, hydrogen is generated on one side of a metal membrane, and a hydrogen detector on the other side is used to measure hydrogen flux. The diffusion of hydrogen in steels is far from straightforward. Since the work of Darken and Smith [9], it is well known that hydrogen trapping in the metal matrix strongly influences its diffusion. Trapping is a phenomenon involving "irregular" sites characterized by stronger hydrogen binding energies in comparison with normal interstitial lattice sites, wherein a hydrogen atom spends a longer average time before eventually jumping out again. The existence of trapping sites makes the interpretation of hydrogen permeation data more difficult since more complicated models are required to understand the diffusion behaviour of hydrogen [10, 11].

This work is focused on understanding trapping and diffusion properties from hydrogen permeation data. Temperature programmed desorption tests are preliminarily performed to establish the type of traps present. Hydrogen permeation tests are subsequently performed and analyzed using different methods critically.

MATERIAL AND METHODS

Enamelling Al-killed IF steels (designation DC06EK according to EN 10027-1 [12]) samples from six different coils, provided by ArcelorMittal, were analyzed in this work: A,B,C,D,E, and F. The typical chemical composition of ArcelorMittal commercial IF enamelling grade steel of this kind is C<50ppm, N<50ppm, S>0.015%, P>0.015%, Mn>0.25%, Si>0.01, 0.05%<Ti<0.1%. The samples were all L = 0.8 mm thick. Metallographic analysis was performed with an optical microscope (Leica DMI3000 M) after Nital 3% etching. Figure 1 shows the ferritic microstructure of the material. Those materials, nominally equal, come from different plants and may have been subjected to different production cycles, thus may exhibit different trapping properties.

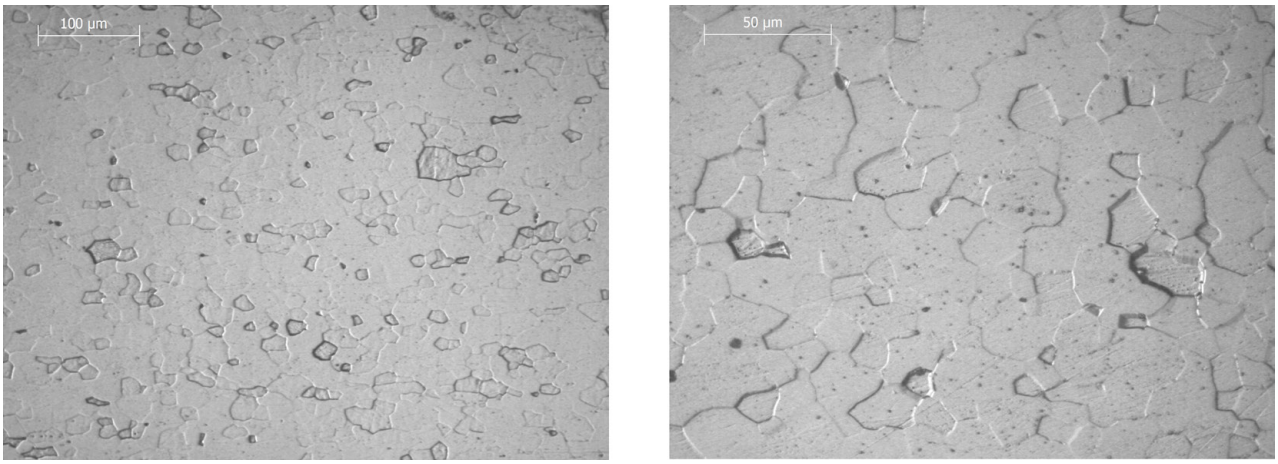

Fig.1 - Typical micrographs of the studied material at low and high magnification. In the high magnification micrograph titanium carbides can be spotted.

TEMPERATURE PROGRAMMED DESORBTION TEST

Temperature Programmed Desorption (TPD) tests were performed on small samples (about 6 g) of the material. The samples were prepared with scotch brite grit and cleaned with ethanol and distilled water. The samples were thereafter weighted and their surface area was measured. Cathodic electrochemical hydrogen charging was performed by putting the samples in a 0.9M CH3COONa, 0.9M CH3COOH, 3.0 % w/w NaCl, 0.3% w/w NH4SCN solution and imposing a 10 mA/cm^2 current density for 60 min. During this process, hydrogen is reduced on the sample surface. Part of this hydrogen

enters the specimen and part combines into hydrogen gas and escapes in the environment. For this material, as confirmed by subsequent permeation tests, 60 minutes charging is enough to assume a homogeneous hydrogen concentration is reached in the sample. After its removal, the specimen was cleaned with distilled water and dried with a cold blow drier. The time required for those operations was always less than 2 minutes. The sample was subsequently inserted into the commercial Helios 3 apparatus [13] in order to perform the TPD test, which entails imposing a linear temperature vs time profile and measuring the escaped hydrogen during the process. Helios 3 employs a solid-state sensor with a controlled airflow for this purpose. The starting temperature of the oven was 50 °C. Samples from coils A, B and C were tested at four different heating rates: 1, 2.5, 5 and 7.5 °C/min. Samples from coils E-G were only tested at 5 °C/min.

HYDROGEN PERMEATION TEST

Hydrogen permeation tests were performed on the studied materials. The samples were prepared with scotch brite grit, cleaned with ethanol and distilled water, and dried with a blow drier. The specimens were subsequently mounted on the commercial Helios 2 apparatus [13]. One side of the specimen was submerged in the hydrogen charging solution (0.9M CH_3COONa, 0.9M CH_3COOH, 3.0 % w/w NaCl, 0.3% w/w NH_4SCN) and a cathodic current density of 10 mA/cm^2 was imposed. The solution and current density were the same of the TPD tests. The other side of the specimen was attached to a hydrogen gas solid-state sensor to measure the hydrogen flux. This apparatus provides a simple and fast setup, suitable for industrial settings. The tests were performed at around 30 °C ambient temperature.

The models most widely employed to rationalize hydrogen diffusion and trapping are McNabb and Fosters' [10], and Oriani's [11] models. McNabb and Foster's model assumes that hydrogen atoms that occupy regular lattice interstitial locations (with concentration C), in addition to their diffusion due to concentration gradient with coefficient D, interact with a certain concentration of traps N, which can be filled. The dynamic of the trap occupancy rate n is governed by the frequency parameters k and p, linked to trapping and detrapping energies.

$$\begin{cases} \dfrac{\partial C}{\partial t} + N\dfrac{\partial n}{\partial t} = -D\dfrac{\partial^2 C}{\partial^2 x} \\ \dfrac{\partial n}{\partial t} = kC(1-n) - pn \end{cases} \qquad \text{(Eq.1)}$$

Oriani's model, by assuming that the local trapped population is always in equilibrium with local lattice hydrogen, is a simplification of the above equations, which ultimately results in a Fick-type law with a diffusion coefficient that depends upon hydrogen concentration:

$$\begin{cases} \dfrac{\partial C}{\partial t} = -D_{eff}(C)\dfrac{\partial^2 C}{\partial^2 x} \\ D_{eff}(C) = \dfrac{D}{1 + \dfrac{N\dfrac{k}{p}}{\left(1 + C\dfrac{k}{p}\right)^2}} \end{cases} \qquad \text{(Eq.2)}$$

Both models show how the apparent diffusivity D_{app} exhibited by the material with hydrogen traps has to be, in general, a function of trap saturation. For this reason, during the same permeation test, the D_{app} may very well change as the hydrogen concentration in the specimen raises up to equilibrium.

Various methods have been proposed in order to estimate the D_{app} value from permeation data:

- Breakthrough time $D_{app} = \dfrac{L^2}{15.3\, t_{br}}$
- Time lag method $D_{app} = \dfrac{L^2}{6\, t_{lag}}$

- 63% method $D_{app} = \frac{L^2}{6\, t_{63}}$
- Fourier fit
- Laplace fit

The breakthrough time t_{br} method estimates the diffusivity from the linear rising transient of the permeation curve: the linear fit of that part of the curve is found and the value t_{br} is taken to be the time of the intercept on the time axis of that fit.
The time lag method t_{lag} focuses on a sort of delay to the steady-state conditions. First, ∫Jdt is plotted against time, then the linear steady-state region is extrapolated to its intercept on the time axis, where the value t_{lag} is found.
Arguably, the simplest method is the t_{63} method, where the data of virtually one single point of the normalized permeation curve is directly used in the calculation: t_{63} is the time corresponding to $\frac{J}{J_\infty}$ =63%. The method stems from observations of Devanathan and Stachursky who observed that value t_{lag} could be easily estimated by looking for t_{63}, a claim that is not true in general, since trapping can strongly change the shape of the curve [8, 14].
The main drawback, jointly shared among each of the common interpretation methods, is their link to Fick's diffusion law. In fact, each method looks for the "closest" Fick permeation curve and claims its diffusivity value to be representative of that of the tested material. Each method essentially proposes a different definition of "closeness", by focusing on different areas of the curve or approximation methods. The same applies to the Fourier or Laplace method, here not considered [14].

Finally, permeation data can also be studied by estimating the parameters of McNabb and Foster's diffusion model. For this purpose, we employed a matlab script solving McNabb and Foster's equations (Eq. 3) with constant concentration boundary conditions. The specimen was assumed to be sufficiently thin, allowing us to solve McNabb and Foster's PDEs using one spatial dimension. For its solution, both Matlab's pdepe routine and a custom backward time-centered space implicit finite difference scheme can be used. The non-linear problem was solved with an iterative approach. Both methods provided the same results for the range of parameters used in this work.
Given a tentative set of parameters, the prediction error can be calculated by taking the square error between predicted and experimental flux for each time step. Matlab's function fminsearch was then used to find the parameters of McNabb and Foster's model better fitting the experimental data.

$$\begin{cases} \frac{\partial C(t,x)}{\partial t} + N\frac{\partial n}{\partial t} = -D\frac{\partial^2 C}{\partial^2 x} \\ \frac{\partial n(t,x)}{\partial t} = kC(1-n) - pn \\ C(0,x) = 0, n(0,x) = 0 \quad 0 < x \le L \\ C(t,L) = 0, n(t,L) = 0 \quad t \ge 0 \\ C(t,0) = C_0 \quad t \ge 0 \end{cases} \qquad \text{(Eq.3)}$$

The hydrogen concentration on the inlet surface was assumed to be equal to $\frac{L\, J_\infty}{D}$, and the parameter D was calculated using:

$$D = 7.23 * 10^{-8} \exp\left(-\frac{5.69 \frac{kJ}{mol}}{RT}\right) \qquad \text{(Eq.4)}$$

Where T is the measured absolute temperature during the test, and R is the real gas constant. The specimen thickness was L=0.8 mm and parameters k, p and N were calculated from the optimisation procedure.

RESULTS

Temperature Programmed Desorbtion Test

Figure 2 shows the results for coils A, B and C. Curves corresponding to faster heating mostly show a higher

peak height located at higher temperatures, as expected. In some cases, incoherent results were found, such as a higher peak flux or peak temperature with a lower heating speed. This is evidence of some experimental error, possibly due to the handling time between charging and the desorption test, or due to microcracking on some specimens. Therefore, TPD data has to be used carefully and only as guidance for further analysis.
What can be ascertained from the test results is that only low to medium energy trap types were detected for each specimen: no high-temperature peak was ever detected.

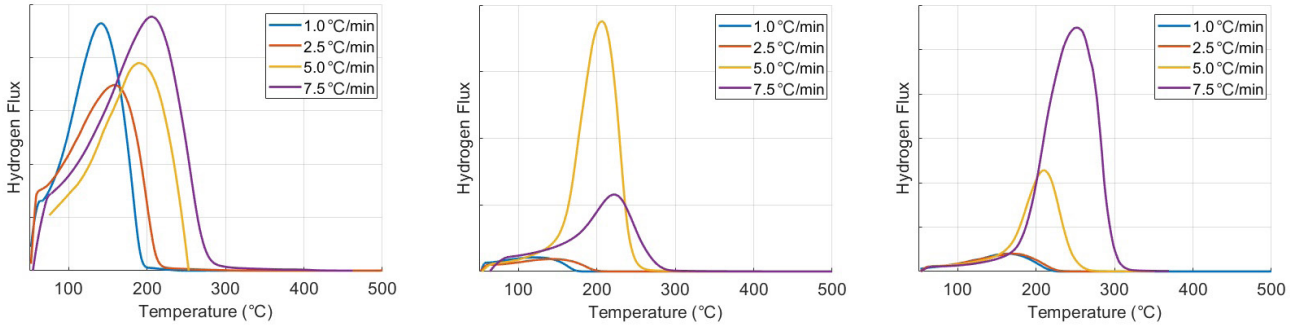

(a) Coil A (b) Coil B (c) Coil C

Fig.2 - Results of Temperature Programmed Desorbtion Tests.

An indicative estimation of the trapping energy can be performed by using Kissinger's formula [15, 16]:

$$\frac{\partial \ln \left(\varphi / T_P^2\right)}{\partial \left(1 / T_P\right)} = -\frac{E_a}{R} \qquad \text{(Eq.5)}$$

where E_a is the detrapping activation energy and T_P is the temperature at which a desorption peak is measured. To identify partially superimposed peaks, gaussian deconvolution is usually employed. With the obtained data, a single-peak deconvolution seems to better fit most curves, but the results are not reliable enough to draw definite conclusions. Figure 3 shows the results of this calculation.
TPD results from coils E-F, here not shown in full for brevity's sake, are similar to results from coils A-C and show no high-temperature peak.

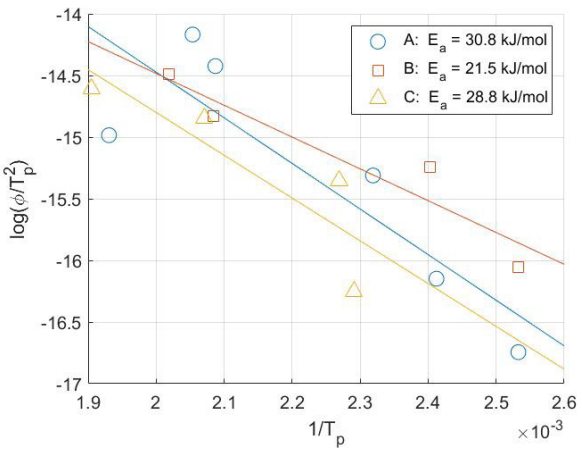

Fig.3 - Results of Temperature Programmed Desorbtion Tests on the Choo-Lee plot.

Hydrogen Permeation Test

Figure 4 shows the results from Hydrogen permeation tests for each coil. Figure 5 graphically shows the different methods used to estimate the diffusivities from permeation data for coil A: the breakthrough method, the time lag method, and the t_{63} method. Table 1 shows the calculated values for D_{app} for each coil. The significant difference among the results obtained from different methods is a telltale sign of the influence of trapping on the transport of hydrogen, and of the general unsuitability of those methods.

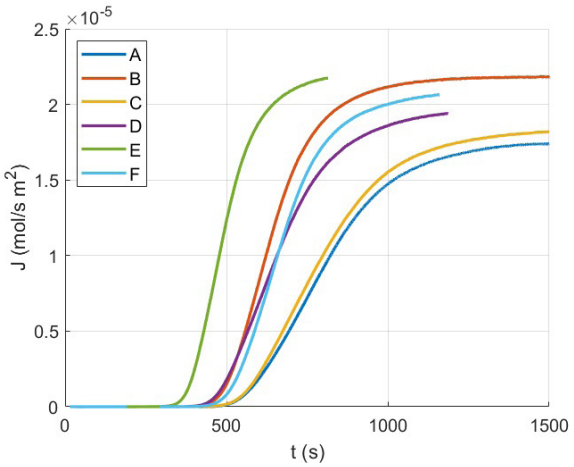

Fig.4 - Results of Permeation Tests.

Tab.1 - Estimation of diffusion and trapping parameters from permeation tests, various D_{app} are measured in m^2/s, the trap binding energy E_b is kJ/mol and traps density N is mol/m^3.

coil	Breakthrough	Time Lag	t_{63}	E_b	N
A	$7.40*10^{-11}$	$1.34*10^{-10}$	$1.28*10^{-10}$	37.0	46.1
B	$8.53*10^{-11}$	$1.65*10^{-10}$	$1.61*10^{-10}$	37.9	29.6
C	$7.59*10^{-11}$	$1.35*10^{-10}$	$1.30*10^{-10}$	37.2	39.5
D	$8.82*10^{-11}$	$1.62*10^{-10}$	$1.56*10^{-10}$	36.2	51.4
E	$1.11*10^{-10}$	$2.19*10^{-10}$	$2.12*10^{-10}$	36.8	34.0
F	$8.15*10^{-11}$	$1.60*10^{-10}$	$1.55*10^{-10}$	36.7	47.2

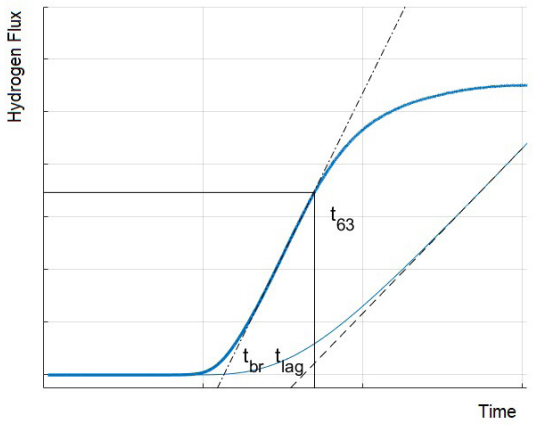

Fig.5 - RInterpretation of permeation data through the breaktrough, time lag and t_{63} method.

Possibly the most thorough method to elaborate permeation data is the comparison with predictions using McNabb and Foster's model. Figure 6 shows the comparison between simulated and experimental curves. The curve reconstruction is almost perfect, and the obtained energy values are coherent among each material. The trap binding energy represents a value that is a bit higher than what is reported for dislocation traps (20 to 30 kJ/mol) in the literature.

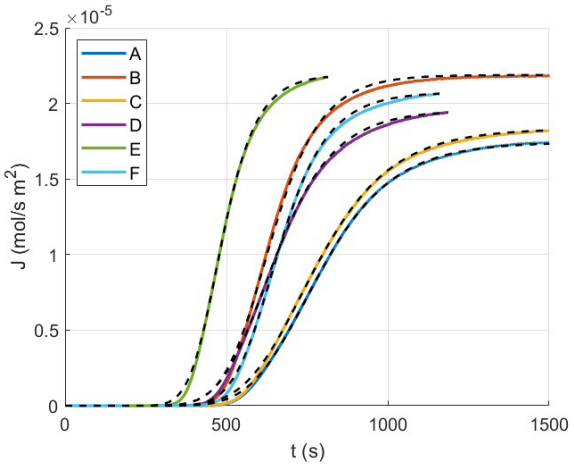

Fig.6 - Results of Permeation tests and simulated permeation curves using McNabb and Foster's model.

DISCUSSION

Data from TPD tests clearly show that only a single type of trap, or at least multiple traps with similar binding energy levels, is activated in the employed charging conditions. The energy estimation is not reliable due to the significant data scatter, but the peak temperatures are clearly compatible with weak traps such as dislocations and grain boundaries.

Permeation tests show how specimens from nominally identical coils can have different properties. The estimation of D_{app}, performed using three different methods commonly found in the literature shows how trapping has influenced the permeation curves due to significant differences, mainly between the breakthrough method and the similar time lag and t_{63} methods. To overcome this problem, McNabb and Foster's equations were solved to find a set of parameters able to reproduce the behaviour of the whole permeation curve. The results show comparable values of trap energy, but the results are higher than those obtained by TPD.

As proposed by Fallahmohammadi et al. [17], one could estimate D_{app} employing the t_{63} method but varying the target value of $\frac{J}{J_\infty}$,thus providing a simple estimation of the apparent diffusivity at different points of the transient curve. For this purpose, the transient solution of a 1D permeation problem for a Fick material is employed:

$$\begin{cases} \dfrac{\partial C}{\partial t} = -D\dfrac{\partial^2 C}{\partial^2 x} \\ C(0,x) = 0, \quad 0 < x \leq L \\ C(t,L) = 0, \quad t \geq 0 \\ C(t,0) = C_0, \quad t \geq 0 \end{cases} \qquad \text{(Eq.6)}$$

The solution of this problem is commonly expressed in terms of normalized flux $\frac{J}{J_\infty}$ and normalized time $\tau_f = \frac{Dt}{L\hat{}2}$ (the expressions in [14] have two printing mistakes, [18] can be used to compare the results):

$$\frac{J}{J_\infty} = \frac{2}{\sqrt{\pi\tau_f}} \sum_{m=1}^{\infty} \exp\left(-\frac{(1+2m)\text{^}2}{4\tau_f}\right) \quad \text{(Eq.7)}$$

or

$$\frac{J}{J_\infty} = 1 + 2\sum_{n=1}^{\infty} (-1)^n \exp\left(-n^2\pi^2\tau_f\right) \quad \text{(Eq.8)}$$

With the use of those expressions, the function $\tau_f = g(\frac{J}{J_\infty})$, that is the normalized time at which Fick's permeation curve reaches the desired normalized flux, can be calculated.

Conversely, for each experimental point $\left(t, \frac{J}{J_\infty}\right)$, only a single solution of Eqs. 6 that intersects the point can be found, and its diffusion coefficient can be calculated by equating $\tau = \frac{t\,D}{L^2} = \tau$:

$$D = \frac{L^2\tau_f}{t} = \frac{L^2}{M\,t} \quad \text{(Eq.9)}$$

where M is t_f^{-1}, thus providing us with an estimation of D_{app} by using the selected experimental point.

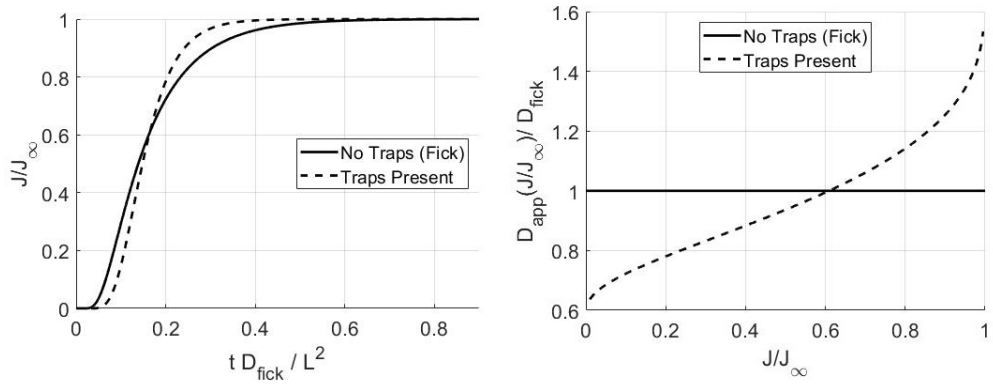

(a) (b)

Fig.7 - Permeation curves (a) and apparent diffusivity vs normalized flux curves according to Eq. 9 (b) for a sample material with and without trapping. The diffusivity of the trap-less material is D_{fick}, equal to D_{63} for the material with traps.

With this procedure, the whole permeation curve $\left(t, \frac{J}{J_\infty}\right)$ can be mapped on a new graph: $\left(\frac{J}{J_\infty}, D_{app}\right)$ Figure 7 (a) shows a characteristic permeation curve for a material with no traps and diffusion coefficient D_{fick}, and one of a material following McNabb and Fosters's model, chosen so that $D_{63\%}$=D_{fick}. Figure 7 (b) shows the D_{app} calculated with the described procedure for both curves. For the Fick curve, the calculated diffusion coefficient is obviously constant on the whole range. On the other hand, the calculation for the material with trapping shows that D_{app} increases during the permeation, as trap occupancy increases.

Figure 8 (a) shows the procedure applied to permeation data from coil A. This figure highlights that the breakthrough method reflects the diffusivity at about 10% flux, and the time lag method reflects the diffusivity at a slightly later stage than the t_{63} method. Due to different trap occupancies at those stages, the D_{app} values are significantly different. As a consequence, a D_{app} measurement that relies upon the first part of the curve

appears to be less adequate to differentiate materials by their permeation properties. The same trend applied to the other coils.

Figure 8 (b) shows the same procedure applied to each permeation curve. Clearly, the curves which exhibited a faster diffusion are placed above, but it can also be observed that they show a higher slope. This can be intuitively explained by using the expression for D_{eff} (Eq. 2). In that framework, D_{eff} increases with increasing C as traps are saturated and thus stop influencing the diffusive behaviour, but the speed of this change is affected by trap density and the energy parameter k/p. With increasing N or decreasing k/p, D_{eff} grows more slowly since more or weaker traps are harder to saturate. Trapping parameters could therefore be estimated from the characteristics of this new $\frac{J}{J_\infty} = D_{app}$ curve. For this purpose, and to make a step towards simplicity and industrial use, only a limited set of points are used: $\frac{J}{J_\infty}$ = 1, 10, 30, 40, 63, 80, and 90 %, the same points highlighted in [17].

Since D_{app} shows a reasonably linear behaviour for each curve, these points are used to fit a line: $D_{app}=D_0+K\frac{J}{J_\infty}$, where D_0 and K are the fitted parameters. Both trap density and trap binding energy have an influence on D_0 and on K but given the, expected, low variability of the calculated values of E_a, N is the parameter that mainly influences D_0 and K. Figure 9 shows the graph of K vs N: the points show a strong linear correlation.

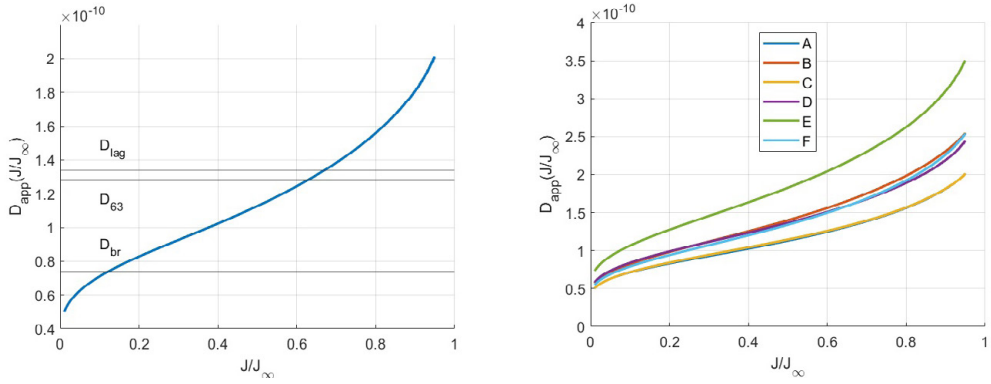

(a) (b)

Fig.8 - Diffusivity calculated at each normalized flux point according to Eq. 9 for coil A (a) and every tested coil (b).

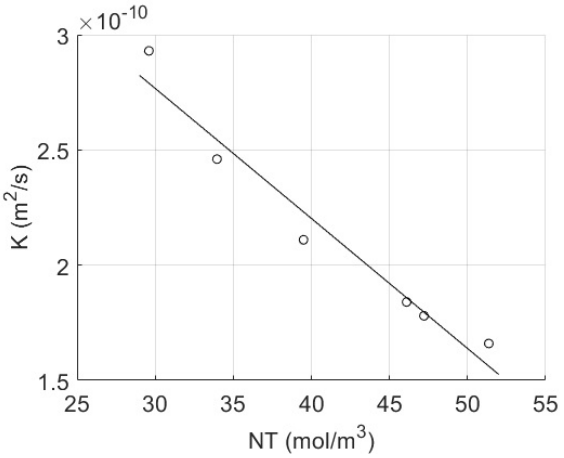

Fig.9 - Slope K of best fit line in the diffusivity/normalized flux ($D_{app} = f\left(\frac{J}{J_\infty}\right)$) graph against trap density according to McNabb and Foster's model.

CONCLUSION

In this work, coils of DC06EK interstitial free steels were studied. Temperature programmed desorbtion tests were performed on hydrogen-charged specimens. Data from those tests showed a single desorption peak for each iteration and material, showing no influence of high-energy trapping. Hydrogen permeation tests were performed. The parameters of McNabb and Foster's diffusion and trapping model that best fitted the experimental data were found, allowing for an estimation of trapping energy and trap density for each material. Results showed a reasonably similar trap energy among all tests, with trap density being the main variable parameter. Commonly used methods to estimate diffusivity from permeation data were used, and their inadequacy was shown. To further explain where their inadequacy lies, the apparent diffusivity at each point $\left(t, \frac{J}{J_\infty}\right)$ of the permeation curve was calculated using the solution of a Fick permeation problem. Results showed that the breakthrough and the time lag methods provide the apparent diffusivity of the permeation data at around 10% $\frac{J}{J_\infty}$ and slightly above 63% $\frac{J}{J_\infty}$ respectively. Finally, the apparent diffusivity at 1, 10, 30, 40, 63, 80, and 90 % $\frac{J}{J_\infty}$ was used to fit a line. The slope of this line was correlated very precisely with trap density for this set of materials, suggesting that, given a sufficiently well-defined applicability range, empiric formulae could be found for specific steel classes or steel designations in order to estimate trap density from this data. Additionally, preliminary numerical investigations show that combined use of the height and slope of the $D_{app}\left(\frac{J}{J_\infty}\right)$ line could help estimate both trap energy and trap density. Further study with a larger sample size is necessary.

BIBLIOGRAPHY

[1] Steel for Enamelling and Enamelled Steel - User Manual, ArcelorMittal.
[2] G. H. Spencer-Strong, "Some examples of the functional use of porcelain enamel and ceramic coatings for Steel," Symposium on Porcelain Enamels and Ceramic Coatings as Engineering Materials, 1954.
[3] M. A. Collins, Atlas of enamel defects, Institute of Vitreous Enamellers, 1995.
[4] W. W. Higgins and W. A. Deringer, "Investigation of fish-scale phenomena," Journal of the American Ceramic Society, vol. 24, p. 383–392, 1941.
[5] Pemco Enamel manual, Pemco International, 2008.
[6] Ente Nazionale Italiano di Unificazione, "UNI EN 10209:2013.," Cold rolled low carbon steel flat products for vitreous enamelling - Technical delivery conditions, 1998.
[7] Ente Nazionale Italiano di Unificazione, "UNI 11734:2018," Determining fish-scale susceptibility of enameling steel, 2018.
[8] M. A. V. Devanathan and Z. Stachurski, "The adsorption and diffusion of electrolytic hydrogen in Palladium," Proceedings of the Royal Society of London. Series A. Mathematical and Physical Sciences, vol. 270, p. 90–102, 1962.
[9] L. S. Darken and R. P. Smith, "Behavior of Hydrogen in Steel During and After Immersion in Acid," Corrosion, vol. 5, p. 1–16, 1949.
[10] A. McNabb and P. K. Foster, "A New Analysis of the diffusion of hydrogen in iron and ferritic steels," Trans. of the metallic Soc., vol. 227, p. 618–627, 1963.
[11] R. A. Oriani, "The diffusion and trapping of hydrogen in steel," Acta metallurgica, vol. 18, p. 147–157, 1970.
[12] Comité Européen de Normalisation, "EN 10027-1:2016," Designation systems for steels - Part 1: Steel Names, 2016.
[13] R. Valentini, Method for Permeation Hydrogen Measurements, European Patent EP2912452B1, 2012.
[14] A. Turnbull, M. S. de Santa Maria and N. D. Thomas, "The effect of H2S concentration and pH on hydrogen permeation in AISI 410 stainless steel in 5% NaCl," Corrosion Science, vol. 29, pp. 89-104, 1989.
[15] H. E. Kissinger, "Reaction kinetics in differential thermal analysis," Analytical chemistry, vol. 29, p. 1702–1706, 1957.
[16] W. Y. Choo and J. Y. Lee, "Thermal analysis of trapped hydrogen in pure iron," Metallurgical Transactions A, vol. 13, p. 135–140, 1982.
[17] E. Fallahmohammadi, F. Bolzoni and L. Lazzari, "Measurement of lattice and apparent diffusion coefficient of hydrogen in X65 and F22 pipeline steels," International Journal of Hydrogen Energy, vol. 38, pp. 2531-2543, 2013.
[18] J. Crank, The mathematics of diffusion, Oxford university press, 1979.

Un nuovo approccio allo studio della permeazione dell'idrogeno in acciai da smaltatura

Gli acciai interstitial free da smaltatura sono comunemente utilizzati in molte applicazioni industriali per la loro resistenza a molti agenti ambientali (corrosivi, abrasivi...), perciò trovano svariate applicazioni, tra le quali il settore degli elettrodomestici oppure in componenti per l'architettura. Uno dei tipici difetti di fabbricazione che possono ritrovarsi in questa famiglia di materiali è il cd. fishscaling, cioè il distacco di parte dello smalto dalla superfice del componente a seguito del processo di smaltatura. Il fishscaling è dovuto all'idrogeno atomico che, penetrato all'interno del materiale durante le varie fasi del processo produttivo, diffonde verso lo smalto il quale, essendo sostanzialmente impermeabile all'idrogeno, determina un punto di accumulo di idrogeno nella interfaccia metallo-smalto. L'idrogeno, se eccessivamente accumulato, determina alla fine una separazione tra i due materiali. Risulta chiaro come la comprensione del fenomeno diffusivo dell'idrogeno nell'acciaio sia un componente fondamentale per la comprensione del fishscaling. Ma il processo diffusivo dell'idrogeno negli acciai è complicato dalla presenza delle trappole, che sono siti (come bordi di grano, interfacce con precipitati, microvuoti o dislocazioni) in cui l'idrogeno si trova in uno stato energetico inferiore ai siti interstiziali regolari; perciò, tenderà a permanervi un tempo sensibilmente più lungo rispetto al tempo medio di salto tra gli stessi siti interstiziali regolari. Un modello matematico che permette di comprendere il fenomeno è il modello di McNabb e Foster, che prevede che l'idrogeno "libero", oltre che diffondere nello spazio seguendo la legge di Fick, possa dinamicamente diventare idrogeno "intrappolato" e viceversa. In questo lavoro, sei campioni da lotti diversi sono stati preliminarmente studiati con la tecnica del desorbimento a temperatura programmata (TPD), per cui a seguito di un caricamento elettrochimico di idrogeno, al provino viene imposta una rampa lineare di temperatura mentre un sensore rileva l'idrogeno che esce dal provino. Questa prova permette di avere una prima caratterizzazione della quantità e tipologia di trappole presenti nel materiale e una stima della loro energia di legame. Successivamente sono state svolte delle prove di permeazione: l'idrogeno generato per via elettrochimica su una superfice del provino tende ad attraversarne lo spessore e viene quindi rilevato da un sensore posto sull'altra superfice. L'andamento temporale del flusso di idrogeno misurato permette quindi di ottenere una caratterizzazione del comportamento diffusivo dell'idrogeno nel provino studiato. In letteratura esistono numerosi metodi utilizzati per stimare una "diffusività apparente" a partire dalle prove di permeazione, metodi che rappresentano un tentativo di condensare in un solo parametro un fenomeno che necessariamente richiede più informazioni per essere caratterizzato, allo scopo di fornire in modo semplice e ripetibile un singolo parametro di riferimento per, ad esempio, la definizione di condizioni contrattuali e parametri per il controllo qualità. Tutti questi metodi si basano alla fine sull'individuazione della diffusività del materiale privo di trappole che determinerebbe la curva di permeazione "più vicina" a quella sperimentale. La differenza sta nel modo in cui questo "più vicina" viene operazionalizzato. In questo articolo sono stati considerati il metodo del breakthrough, del time lag e del t_63. Quest'ultimo consiste nel ricercare il tempo dall'inizio della prova, appunto t_63, in cui il flusso misurato abbia raggiunto il 63% del flusso a regime. Per ottenere un modello che riesca a ricostruire al meglio la reale curva sperimentale, abbiamo fatto uso del modello di McNabb e Foster, che ci ha permesso di ottenere una stima della densità delle trappole e della loro energia per i vari provini. I risultati (evidenziati in Tabella 1) mostrano come l'energia delle trappole ottenuta sia omogenea per tutti i materiali, come atteso essendo tutti nominalmente uguali, ma la densità delle trappole risulti diversa, determinando quindi la misurata differenza nelle diffusività apparenti. La rielaborazione del metodo del t_63, proposta da Fallahmohammadi et al, permette di ottenere una stima della diffusività apparente a partire, in generale, da ogni valore percentuale di flusso rispetto al flusso a regime, ed è stato qua inizialmente impiegato per evidenziare l'effetto delle trappole. La Figura 8 mostra come la presenza di trappole de-

termini un progressivo aumento della diffusività apparente mentre il flusso misurato aumenta. Questo procedimento è stato applicato a tutte le prove svolte, ed è stato osservato come le curve che mostravano una diffusione più veloce mostravano anche una maggiore differenza tra la diffusività apparente ottenuta da bassi valori di flusso rispetto a quelli ottenuti da valori più alti. Questo effetto, giustificabile partendo da uno studio effettuato da Oriani, può essere usato per offrire un metodo alternativo per la stima della densità di trappole a partire dalle prove di permeazione, utilizzando comunque una procedura semplice e ripetibile: cioè una relazione tra la variazione della diffusività apparente con il progressivo aumento di flusso misurato, valida chiaramente solo all'interno della ristretta cerchia di materiali considerati. Con la quantità limitata di prove effettuate per questo lavoro una relazione lineare sembra adeguata a tale scopo, come mostrato in Figura 9.

TORNA ALL'INDICE >